ISSN 0006-2979, Biochemistry (Moscow), 2012, Vol. 77, No. 6, pp. 648-658. © Pleiades Publishing, Ltd., 2012.
Original Russian Text © V. B. Saprunova, M. A. Lelekova, N. G. Kolosova, L. E. Bakeeva, 2012, published in Biokhimiya, 2012, Vol. 77, No. 6, pp. 796-808.

SkQ1 Slows Development of Age-Dependent Destructive Processes in Retina and Vascular Layer of Eyes of Wistar and OXYS Rats

V. B. Saprunova[1,2]*, M. A. Lelekova[1], N. G. Kolosova[2,3], and L. E. Bakeeva[1,2]

[1]Belozersky Institute of Physico-Chemical Biology, Lomonosov Moscow State University, 119234 Moscow, Russia; fax: (495) 939-3181; E-mail: fxb@belozersky.msu.ru
[2]Institute of Mitoengineering, Lomonosov Moscow State University, 119992 Moscow, Russia; fax: (495) 939-5945; E-mail: info@mitotech.ru; saprunova@mail.genebee.msu.ru
[3]Institute of Cytology and Genetics, Siberian Branch of the Russian Academy of Sciences, pr. Akademika Lavrentieva 10, 630090 Novosibirsk, Russia; fax: (383) 333-1278

Received February 23, 2012

Abstract—We show the development of clearly pronounced age-related pathological changes in eye tissues of Wistar and OXYS rats. Photoreceptor cells were virtually absent in all OXYS rats in the age of 24 months. Massive accumulations of lipofuscin granules were detected in the pigmented epithelium cells. Flattening, overgrowing, and degradation of endothelial cells of choriocapillaries were also observed. Along with these changes, vessels without signs of degradation were detected in the pigmented epithelium. In 24-month-old Wistar rats these changes were local and were seen in only some of the animals. The mitochondria-targeted antioxidant SkQ1 (the rats were given SkQ1 daily with food at the dose of 250 nmol/kg for 5 months, starting from the age of 19 months) prevented the development of these pathological changes in both Wistar and OXYS rats. The data were subjected to mathematical processing and statistical analysis.

DOI: 10.1134/S0006297912060120

Key words: ultrastructure, oxidative stress, retina, choriocapillary layer, antioxidant

Decrease in the sight and its loss in older people are mainly caused by age-related macular degeneration (AMD). It is a complex disease caused by specific changes in the choriocapillary layer and retina – the retinal pigmented epithelium (RPE) and Bruch's membrane. However, mechanisms triggering the transition of normal age-related changes to pathology are still unclear. The loss of sight is immediately caused by neovascularization, i.e. growth of anomalous vessels from the eye vascular layer (choroid) into the depth of the retina that finally leads to its detachment.

There are some hypotheses that explain the development of pathological changes in the retina. According to one of these hypotheses, the process is underlain by vascular pathology that leads to disorders in the nourishment of the central zone of the retina that is responsible for sight. Another hypothesis supposes that the flattening, overgrowing (obliteration) of the choroid vessels, and degradation of photoreceptor cells is caused by atrophy of the pigmented epithelium (PE) cells [1-5]. The development of AMD is associated with hypoxia and inflammation [6, 7]. Oxidative stress, i.e. disorders in the balance between the systems of generation and detoxification of reactive oxygen species (ROS), is mainly responsible for the damage [8-12]. The retina utilizes significantly more oxygen than any other tissue because it is constantly under the influence of radiation. The probability of development of oxidative stress is increased, as well as the saturation of photoreceptor membranes and of the PE cells by easily oxidized lipids (to 50% of polyunsaturated fatty acids [13]). The phagocytosis and processing of photoreceptor outer segments in RPE are associated with the enzymatic generation of ROS. Oxidized lipids and cell components are accumulated in the RPE cells with age, and this is accompanied by an excess accumulation of

Abbreviations: AMD, age-related macular degeneration; BM, Bruch's membrane; CCL, choriocapillary layer; INL, inner nuclear layer; IRL, inner reticular layer; LG, lipofuscin granules; ONL, outer nuclear layer; ORL, outer reticular layer; PE, pigmented epithelium; PRL, photoreceptor layer; RL, rod layer; ROS, reactive oxygen species; RPE, retinal pigmented epithelium.

* To whom correspondence should be addressed.

lipofuscin granules (LG) [14]. In the lipofuscin granules ROS are mainly produced by A2E (N-retinol-N-retinylidene ethanolamine). Its accumulation is considered to be a key factor provoking development of AMD [15].

Creation of biological models of human diseases is a promising approach for elucidating of etiology and pathogenesis and also the development of new treatments. In particular, AMD can be induced in the OXYS rat line created at the Institute of Cytology and Genetics, Siberian Branch of the Russian Academy of Sciences (ICG SB RAS) as a model of genetically-determined premature senescence [14, 16-20]. This line is registered in the Rat Genome International Database (http://rgd.mcw.edu).

Retinopathy clinically similar to initial stages of AMD appears in 100% of OXYS rats already by the age of 3-4 months, whereas in Wistar rats similar changes are observed only in 7% of the animals after the age of 12 months. Antioxidants can prevent or slow the development of phenotypic manifestations of the premature senescence in OXYS rats, and their effectiveness is associated with the ability to prevent disorders in mitochondria functioning that are specific for OXYS rats [21, 22]. We found earlier that the mitochondria-targeted antioxidant SkQ1 (plastoquinone-decyl-triphenyl phosphonium) in nanomolar concentrations prevented some manifestations of the accelerated senescence of eye tissues in OXYS rats. Addition of SkQ1 to the diet starting from the age of 8 months completely prevented the development of cataract and retinopathy in OXYS rats observed until the age of one year [14, 16].

Results of studies performed on one-year-old animals presented in the above-mentioned works did not reveal the full spectrum of pathological changes that developed later. Notwithstanding the accelerated senescence observed in OXYS rats, these animals did not reach the terminal stage of age-related disease by the age of 1 year. Therefore, it was very urgent to analyze the state of the retina, PE, and choroid (choriocapillary layer) in OXYS and Wistar rats in the course of senescence and also to study the therapeutic effect of SkQ1 on the age-related pathologies. Thus, the present study was performed on 24-month-old OXYS and Wistar rats that were treated with SkQ1 starting from the age of 19 months. The purpose of this work was to study ultrastructure of the retina, PE, and choroid of 24-month-old OXYS and Wistar rats and to assess the therapeutic effect of SkQ1 on the development of age-related pathological changes in the eye tissues of Wistar and OXYS rats.

MATERIALS AND METHODS

Animals. The development of a complex of premature senescence signs in OXYS rats was a result of directed selection for early spontaneous cataract [23]. In the first five generations cataract development was provoked by a galactose-enriched diet [24]. Now we have the 98th generation of OXYS rats with spontaneous cataract and linked hereditable syndrome of premature senescence that is manifested by retinopathy. The present work was performed on male Wistar (n = 15) and OXYS (n = 15) rats from the ICG SB RAS Collective Use Center "Gene Pools of Experimental Animals". The animals were kept in groups of five rats under conditions of natural illumination, temperature of 22 ± 2°C, and water and food (PK-120-1, Ltd, Laboratorsnab, Russia) *ad libitum*. To monitor age-related changes in the retina, five each Wistar and OXYS rats at the age of 3 months were used. To study the effect of SkQ1 on the development of retinopathy, the Wistar and OXYS rats at 19 months of age were randomly divided into two groups each including five animals: one group was used as the control, whereas the other group was given SkQ1 (250 nmol/kg) with food daily for five months. All procedures were performed in accordance with the European Communities Council Directive No. 86/609/EES.

Electron microscopy. For electron microscopic study, the material was fixed with 3% solution of glutaraldehyde in buffer (pH 7.4) for 2 h at 4°C, then in 1% solution osmium tetroxide in buffer for 1.5 h, and then dehydrated in alcohol solutions with increasing concentrations of ethanol (70% ethanol was saturated with uranyl acetate). The material was flooded in Epon-812 epoxide resin. Serial ultrathin sections were made using a Leica ultramicrotome (Leica Microsystems). The resulting preparations were viewed and photographed using a HU-12 electron microscope (Hitachi, Japan).

Mathematical processing and statistical analysis. In addition to the visual examination of ultrastructure of the central eye area, the electron micrographs were subjected to mathematical processing and statistical analysis. For each animal (five animals in each group) two regions of the retina were obtained (serial sections of electron micrographs) that consisted, on average, of 20 micrographs (mean length of the region was 210 μm). The mathematical processing was performed with the Adobe Photoshop graphic program.

In the first stage all vessels of the choriocapillary layer (CCL) were separated manually, and their sectional area was calculated in pixels. The Bruch's membrane (BM) length was measured. Then the program calculated the ratio of these values and the results were normalized to the BM length (square micrometers per length in micrometers). The statistical parameters were calculated with the STATISTICA 6 program.

RESULTS

Ultrastructure of retina and choroid of 3-month-old Wistar and OXYS rats. The retina of 3-month-old Wistar and OXYS rats has a similar ultrastructure without signs of pathology.

Figure 1 presents a part of the peripheral region of the retina and the adjacent layer of choriocapillaries from

the eye of a 3-month-old rat. One can see the following: the basal part of the photoreceptor layer (PRL), i.e. the layer of rods; the monolayer pigmented epithelium (PE); Bruch's membrane (BM), which is an extracellular complex located between the PE and CCL and consisting of two collagen-enriched layers, the inner and outer ones, which are separated by a central region of elastin and elastin-bound proteins; CCL vessels. Inside the vessel one

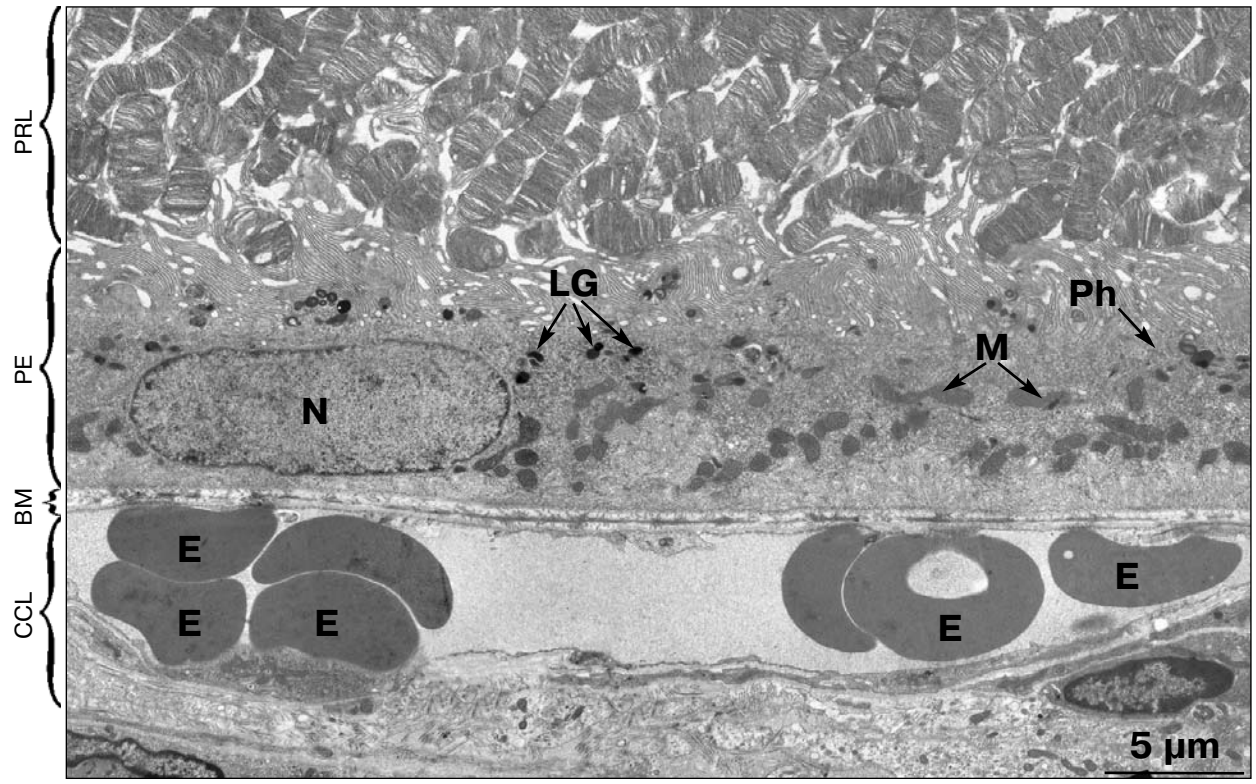

Fig. 1. Ultrastructure of peripheral retina of a 3-month-old Wistar rat. N, nucleus of a PE cell; Ph, phagosome; LG, lipofuscin granules; M, mitochondria; E, erythrocyte; CCL, choriocapillary layer; BM, Bruch's membrane; PE, pigmented epithelium; PRL, photoreceptor layer.

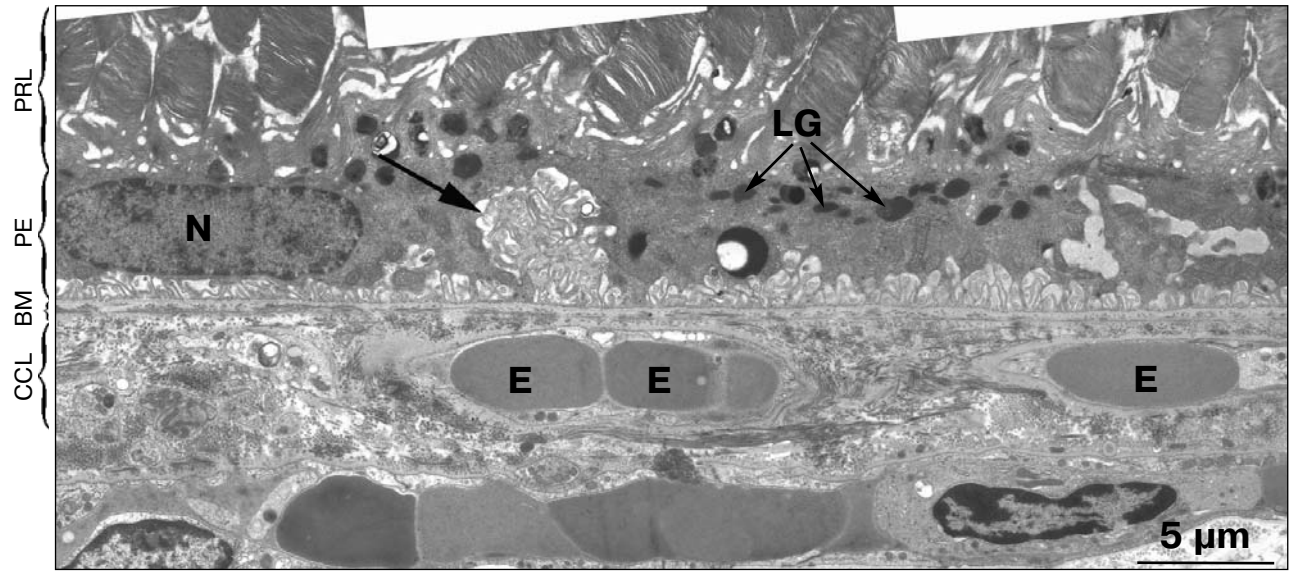

Fig. 2. Ultrastructure of peripheral retina of a 24-month-old Wistar rat. N, nucleus of PE cell; LG, lipofuscin granules; E, erythrocyte. CCL, choriocapillary layer; BM, Bruch's membrane; PE, pigmented epithelium; PRL, photoreceptor layer. The arrow indicates the basal membrane that produces elongated outgrowths of strange shape.

can see erythrocytes. The morphology of the PE cells is characterized by the presence of numerous electron-dense formations in the apical part of the cytoplasm. In the modern literature [25-27], these structures are believed to be lipofuscin granules (LG). Moreover, in the apical zone of the cytoplasm of the PE cells phagosomes are frequently observed formed by packs of worked out discs of photoreceptor membranes of outer segments of cells of the rods phagocytized by the pigment epithelium.

The retina and choroid of a 3-month-old Wistar rat are similar in structures.

Ultrastructure of retina and choroid of a 24-month-old Wistar rat. We found various pathologic changes in 24-month-old Wistar rats in photoreceptor cells, PE cells, BM, and CCL. Figure 2 presents a typical picture of the ultrastructure. The ultrastructure of the retina was not homogenous studied rats. The PE was specified by changes in the basal membranes, which produced elongated strange-shaped outgrowths extending to the rod layer (arrow in Fig. 2). In the apical part of the PE cells there was a massive layer of LG. In some cells of the PE, extremely large LG were present, comparable in size with the nucleus [14]. BM retained its normal ultrastructure. However, large regions of degenerative changes were found in the retina, which occupied the area from the inner reticular layer (IRL) – the zone of location of synapses of the secondary neuron axons with the ganglion neuron dendrites – to the PE cells (Fig. 3). All layers of

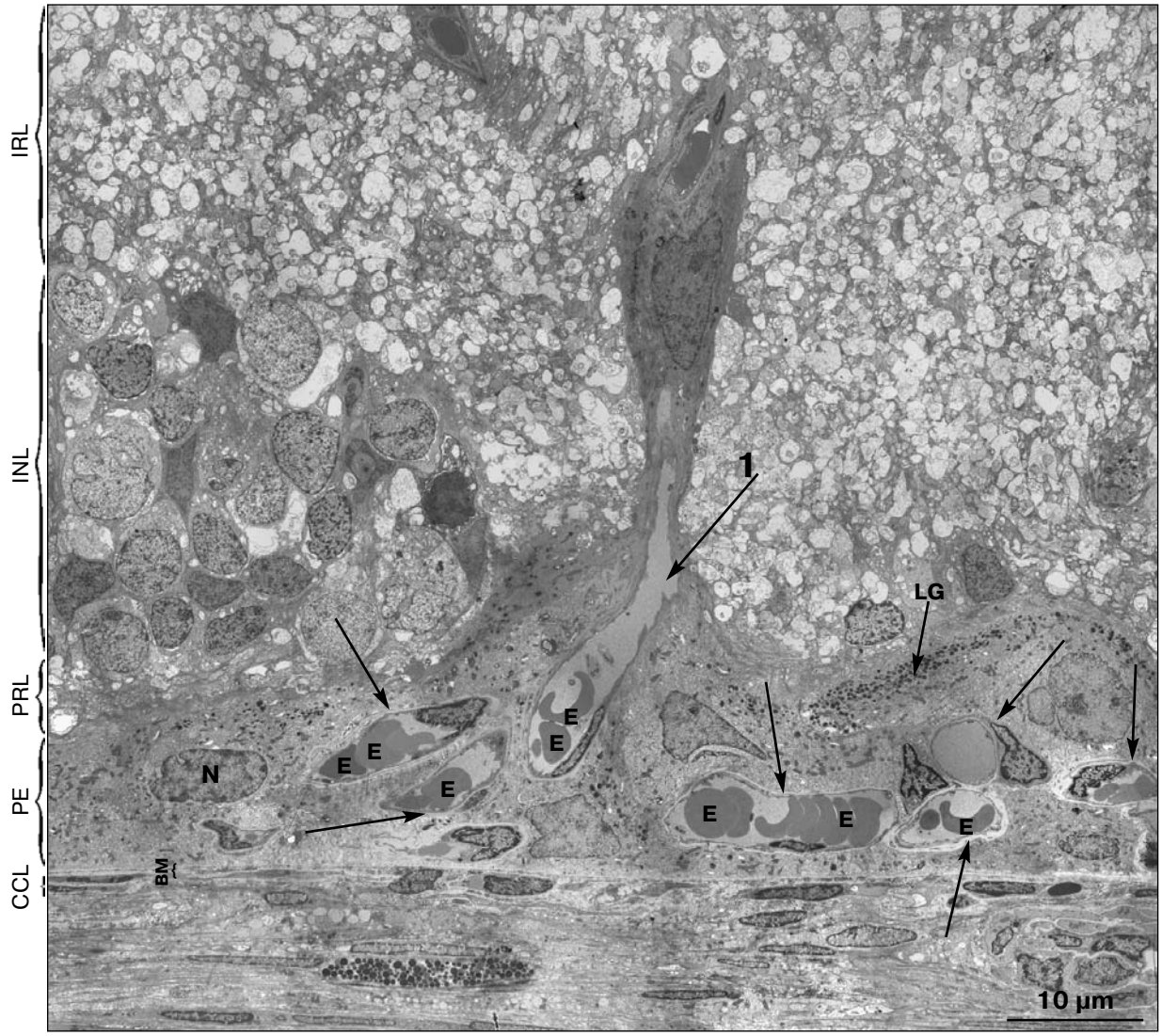

Fig. 3. Electron micrograph of retina region of the eye of a 24-month-old Wistar rat. IRL (inner reticular layer) – the zone of synapses of the second neuron axons with ganglion neuron dendrites; INL (inner nuclear layer) – contains bodies and nuclei of inserted neurons; PRL, photoreceptor layer; PE, pigmented epithelium; CCL, choriocapillary layer; N, nucleus of PE cell; LG, lipofuscin granules; E, erythrocyte. Arrow 1 indicates a blood vessel directed into the layer of PE cells from the retina inner side. Other arrows indicate numerous sections of capillaries in the layer of PE cells.

the retina displayed signs of degradation. A powerful wide outer nuclear layer (ONL) produced by bodies and nuclei of photoreceptor cells was absent, and only individual cells were retained. Cells of the rods were completely lost, and their place was occupied by outgrowths of the cytoplasm of the PE cells (Fig. 3). The PE cells had pronounced pathological changes in ultrastructure: changes in cell shape, increased layer of LG, expansion of basal folds, and vascularization (arrows in Fig. 3). The size of the PE cells was pronouncedly increased (Fig. 1). Virtually complete disappearance of photoreceptor cells resulted in disorders of the tight packing of the retina layers, and this led to an increase in volume of the PE cells. It was especially noticeable due to the shape of nuclei: they were roundish, whereas normally they are flattened and elongated (Fig. 1).

The vascularization of the PE layer cells that we observed is an important sign of pathology developing in the retinal tissue (Fig. 3). The photo presents a completely shaped vessel outgrowing into the layer of PE cells from the inner side of the retina (indicated by the arrow 1 in Fig. 3). The wall of this vessel is formed by the endothelial cell, its inner space is fully filled in, and inside the vessel erythrocytes can be seen. Moreover, numerous sections of capillaries are seen in the PE (they are indicated by other arrows).

Changes in the CCL were found in all animals (Figs. 2 and 3). The number of choriocapillaries was significantly decreased. The atrophy of endothelial cells resulted in obliteration of vessels in the CCL, and the vessel lumens were markedly narrowed. We observed such structure of the CCL in all 24-month-old Wistar rats.

Effect of SkQ1 on ultrastructure of retina and choroid of 24-month-old Wistar rats. No change in the general structure of the retina was detected in Wistar rats treated with SkQ1 during 5 months starting from the age of 19 months. Figure 4 presents a region of the retina of a 24-month-old Wistar rat treated with SkQ1. The picture shows that the retina contains layers normally characteristic for this tissue: the rod layer (PRL) is well pronounced, and photoreceptor cells are covered by PE cells. The PE, BM, and CCL have no significant changes in ultrastructure.

The most demonstrative result of the treatment of rats with SkQ1 was the state of the CCL, which in 24-month-old Wistar rats had no significant differences from the state of choriocapillaries observed in 3-month-old rats of this line (Fig. 5). The photo presents normally shaped choriocapillaries without signs of endothelial cell degradation. Normal blood circulation occurs inside the vessels. Thus, the structure of capillaries in the SkQ1-treated animals corresponded to the state of choriocapillaries observed in 3-month-old animals. Endothelial cells with ultrastructure similar to that of endothelial cells of intact animals are clearly seen.

Mathematical processing and statistical analysis. The electron microscopy data were subjected to mathematical processing and statistical analysis. For each of the three groups of Wistar rats (3-month-old rats, control 24-month-old rats, and 24-month-old rats treated with SkQ1) the mean area of the CCL vessels per 1 μm of BM length was calculated (see "Materials and Methods"). The statistical analysis included 10 regions of the retina for each group of animals. The mean length of the region

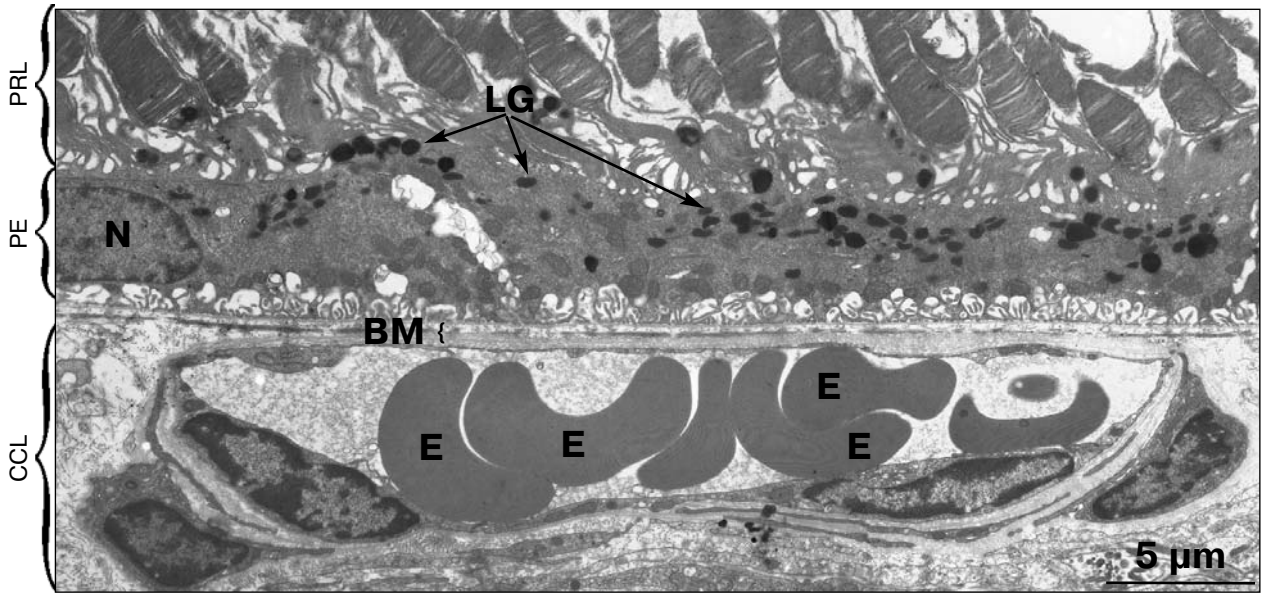

Fig. 4. Ultrastructure of peripheral retina of a 24-month-old Wistar rat that received SkQ1 (250 nmol/kg) daily with food for 5 months. PRL, photoreceptor layer; PE, pigmented epithelium cells; CCL, choriocapillary layer; N, nucleus of PE cell; LG, lipofuscin granules; BM, Bruch's membrane; E, erythrocyte.

was 210 μm, which is near the dimensions in the photos obtained by light microscopy.

The results are presented in Fig. 5. In 24-month-old Wistar rats, the area of choriocapillaries per unit of BM length is more than 3 times lower than in the 3-month-old rats (1.08 ± 0.22 $\mu m^2/\mu m$ as compared to 4.88 ± 1.1 $\mu m^2/\mu m$), which suggests a significant degradation of the choroid vessels. The treatment with SkQ1 had a powerful protective effect; it prevented and/or decreased destructive changes: the area of choriocapillaries per unit of Bruch's membrane length in these animals was 2.22 ± 0.35 $\mu m^2/\mu m$. Thus, the mathematical processing and statistical analysis completely confirmed the visual observations.

Ultrastructure of retina and choroid of a 24-month-old OXYS rat. Pronounced pathological changes in the retina outer layers, BM, and CCL occur in 24-month-old OXYS rats. Figure 6 presents a segment of the retina of a 24-month-old OXYS rat. Degenerative changes of the visual part of the retina occupy the area from the inner nuclear layer (INL) where bodies and nuclei of inserted neurons are located to the cells of PE. Photoreceptor cells are lost nearly completely – only individual nuclei of photoreceptor cells can be seen in the photograph. In the place of the rod layer, there are outgrowths of the cytoplasm of the PE cells. A rather large blood vessel is located in the outer reticular layer (arrow 1 in Fig. 6). Considering its location, this vessel cannot be a choroid vessel or a vessel of the system of the retina central artery, which is another system of blood provision of the eyeball penetrating into it through the optic nerve disc and responsible for nutrition of the inner layers of the retina. The appearance of a vessel in the outer layer of the retina seems to be associated with degradation of the inner retina that allows the vessels to emigrate from the retina inner layers.

In the PE cells of these animals, we found pronounced pathological changes in the ultrastructure: an increase in the layer of LG, growth of basal folds of the PE cells, atrophy of some cells, and vascularization (Figs. 6 and 7). Figure 6 shows an intense layer of LG that occupies the greater part of the cytoplasm of the PE cells. Arrows 1 and 2 in Fig. 7 indicate vessels that are located in the PE cell layer.

We also found that in 24-month-old OXYS rats the BM structure was changed: there were disorders in locations of the collagen and elastin layers. Pathological changes were also detected in the CCL. Pronounced displacements of the BM collagen layers into the region among the CCL vessels resulted in fibrosis of choriocapillaries. The number of choriocapillaries was significantly decreased. The atrophy of endothelial cells resulted in obliteration of vessels of the CCL: the vessel lumen virtually fully disappeared. The earlier location of a choriocapillary could be determined only by location of the nucleus of the endothelial cell that earlier belonged to the vessel wall (Fig. 7).

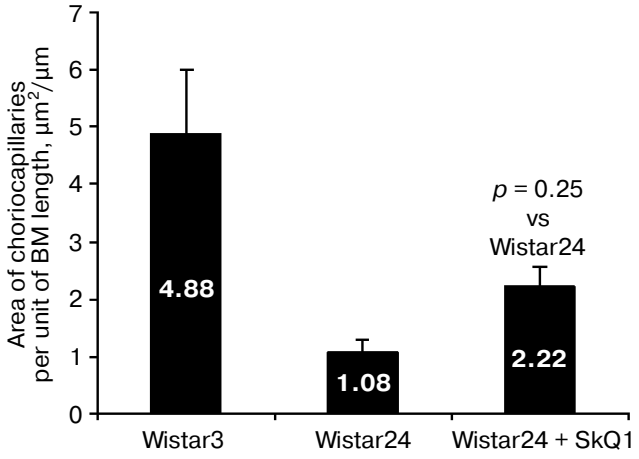

Fig. 5. Area of choriocapillaries per unit of BM length ($\mu m^2/\mu m$) in 3-month-old Wistar rats (Wistar 3), 24-month-old Wistar rats (Wistar 24), and 24-month-old Wistar rats treated with SkQ1 (Wistar 24 + SkQ1) ($p = 0.025$, STATISTICA 6).

Thus, in 24-month-old OXYS rats we have revealed pronounced changes in the ultrastructure: 1) of photoreceptor cells (the layer of rods virtually disappeared); 2) of PE cells: massive accumulations of LG in the cytoplasm of the PE cells, growth of basal folds of the PE cells, atrophy of individual cells, vascularization; 3) of choriocapillaries: obliteration of choriocapillaries, atrophy of endothelial cells, a decrease in the lumen of functioning vessels.

Effect of SkQ1 on ultrastructure of retina and choroid of 24-month-old OXYS rats. In the animals of this group the ultrastructure of the retina was very different of that of OXYS rats untreated with SkQ1. Figure 8a presents a region of the retina from an SkQ1-treated OXYS rat. One can see that the retina contains layers that are normally characteristic for this tissue: the outer nuclear layer (ONL) that includes bodies and nuclei of photoreceptor cells; well developed rod layer (RL) but discriminated from the normal layer by a slight disorganization and fragmentation of some photoreceptors. The layer of photoreceptor cells is covered by cells of the PE.

Note that the retina of OXYS strain rats treated with SkQ1 was not homogenous in structure. Regions with the well-developed layers of photoreceptor cells were present in the same eye alongside regions with degraded layers. However, despite the presence of regions with degraded photoreceptor cells, the retina of the OXYS rats treated with SkQ1 retained ultrastructure close to the normal retina.

Note that ultrastructure of the PE, BM, and CCL of the SkQ1-treated OXYS rats had similar features in all animals studied and did not depend on disorders in the layers of photoreceptor cells. Figure 8b shows that the PE does not have signs of pathology: the cells display well-developed endoplasmic reticulum, and in the cytoplasm

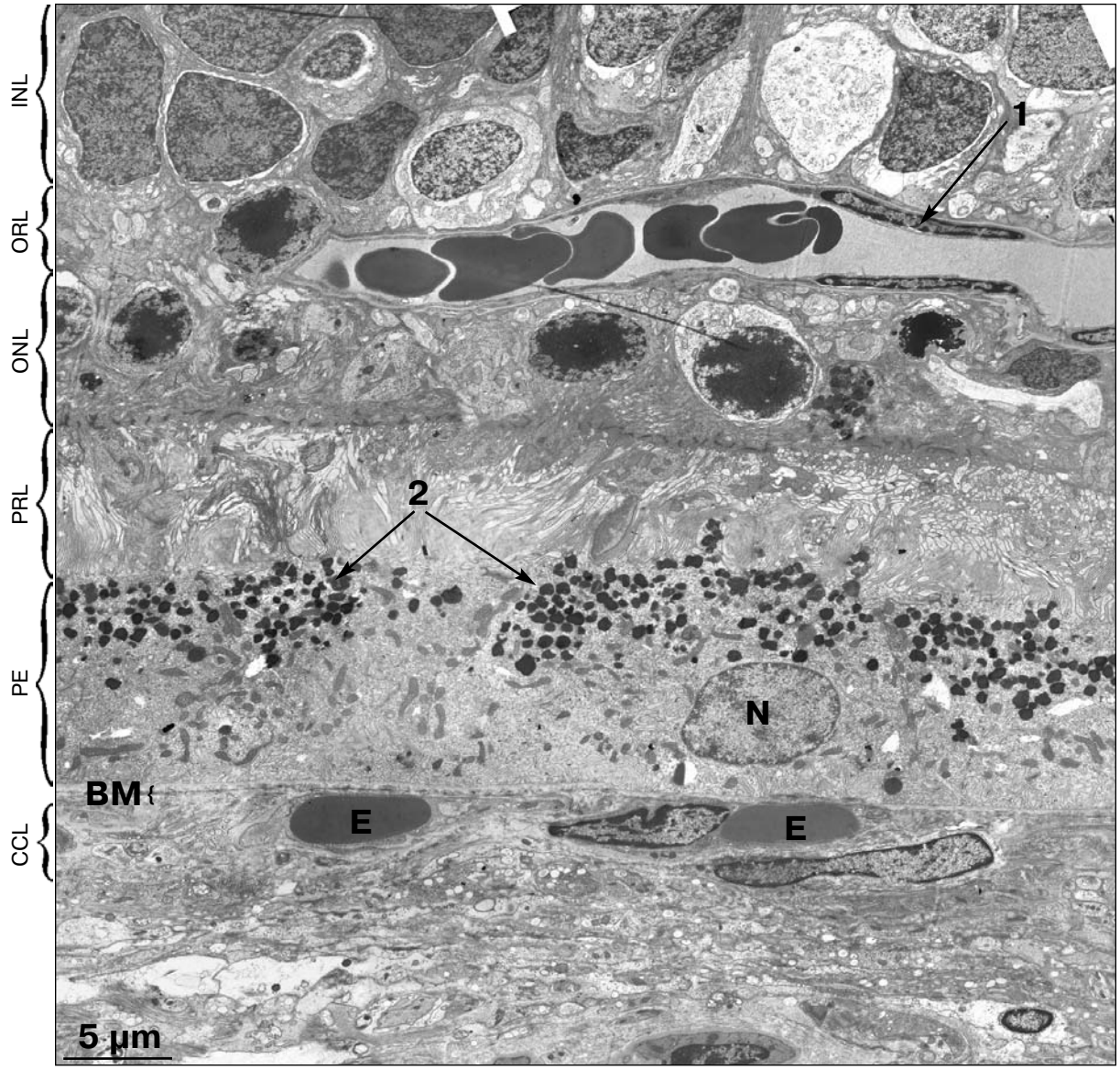

Fig. 6. Electron micrograph of a region of the retina of the eye of a 24-month-old OXYS rat. INL, inner nuclear layer containing bodies and nuclei of inserted neurons; ORL, outer reticular layer – zone of contacts of photoreceptor neuron axons with inserted neuron dendrites; ONL, outer nuclear layer including bodies and nuclei of photoreceptor cells; PRL, photoreceptor layer; PE, pigmented epithelium; CCL, choriocapillary layer; N, nucleus of PE cell; E, erythrocyte; BM, Bruch's membrane. Arrow 1 indicates a blood vessel. The arrows 2 indicate an intense layer of lipofuscin granules.

ribosomes are distinct. The mitochondrial volume is significantly increased: elongated organelles with an intense system of cristae are present.

The treatment of animals with SkQ1 also restored the BM structure. Figures 8a and 8b shows that BM of the SkQ1-treated rats has ultrastructure slightly differentiated from the normal one but does not have anomalous formations (thickenings, protuberances produced by BM basal surface).

Along with the restoration of BM, the treatment with SkQ1 induced recovery of the CCL covering the PE cells (Fig. 8a). While in the control 24-month-old OXYS rats only singular capillaries were present in the choroid and frequently at the whole length of the section (210 μm on average) no vessels occurred, in the SkQ1-treated rats the capillary lumen was distinct, as well as endothelial cells with ultrastructure similar to that of endothelial cells of intact choriocapillaries (Fig. 8a).

Mathematical processing and statistical analysis of electron micrographs were performed for intact OXYS rats at the age of three and 24 months and also for 24-month-old OXYS rats treated with SkQ1 for five months (see "Materials and Methods"). The statistical analysis included 10 regions with length of 210 μm on average for

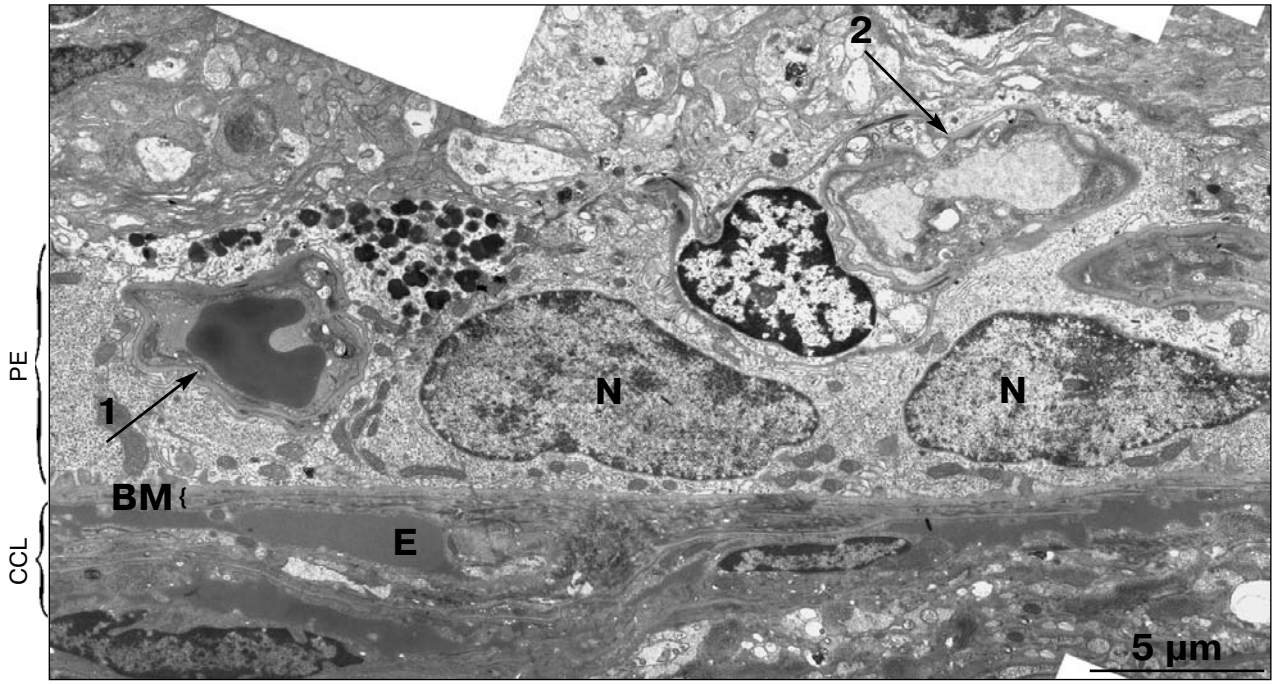

Fig. 7. Electron micrograph of PE, BM, and CCL of a 24-month-old OXYS rat. PE, pigmented epithelium; CCL, choriocapillary layer; E, erythrocyte; N, nucleus of PE cell; BM, Bruch's membrane. Arrows indicate vessels: 1) a vessel located inside the layer of PE cells; 2) a vessel directed into the layer of PE cells from the inner retina side.

each group of animals. Figure 9 shows that in 24-month-old OXYS rats the area of choriocapillaries per unit of BM length is significantly decreased compared to 3-month-old OXYS rats (from 3.04 ± 0.23 to 0.6 ± 0.13 $\mu m^2/\mu m$), which indicates a virtually complete degradation of the choroid vessels. Treatment with SkQ1 for 5 months had a pronounced therapeutic effect: destructive changes in the CCL were prevented. The specific area of choriocapillaries in the SkQ1-treated rats was nearly threefold higher than in the OXYS rats untreated with SkQ1 (1.73 ± 0.21 and 0.6 ± 0.13 $\mu m^2/\mu m$, respectively). This result fully confirms the visual observations.

DISCUSSION

Thus, we have found that in 24-month-old Wistar rats pronounced age-related destructive changes in eye tissues are observed, but these changes are local and do not occur in all animals of this group. As discriminated from Wistar rats, progressing pathological changes in the retina are observed in all 24-month-old OXYS rats, and these changes also affect photoreceptor cells, PE cells, BM, and the CCL.

Vascularization of the PE cells (Figs. 3, 6, and 7) is an important pathological sign revealed by us. On degeneration of the photoreceptor cells, the ONL and RL disappear, and this results in vascularization of the PE cells. According to classical ideas about vessel outgrowing in the case of retina dystrophy, the choroid is a source of capillaries in the PE cells. However, our findings suggest that another source of vascularization can exist. Because of degradation of the outer retina layer, blood vessels from the inner retina immigrate into the PE cells. And on the immigration inside the layer of the PE cells, the capillary starts to increase in size. We are the first to show on the ultrastructural level the vessel outgrowth into the PE cell layer. In fact, Fig. 3 shows that the vessel indicated by arrow 1 is directed into the layer of the PE cells from the inner retina side. And no changes in BM structure associated with the capillary growth from the choroid side are detected.

Obviously, the changes found by us in the PE cell ultrastructure of 24-month-old Wistar and OXYS rats characterize disorders in visual functioning. Thus, according to usual concepts, in the cells of rods during the phototransformation in rhodopsin of *trans*-retinal in a complex with phosphatidyl ethanolamine is transferred across the photoreceptor membrane into the cytoplasm of the outer segment and further into the PE cell [28-30]. In disorders of the visual cycle, retinal not removed in due time from the disc photoreceptor membrane is accumulated inside it and then interacts with phosphatidyl ethanolamine producing in the membrane *bis*-retinylidene-phosphatidyl ethanolamine (A2E-PE), which is a precursor of *bis*-retinylidene ethanolamine (A2E) – the main fluorophore of LG. It seems that the massive accumulation of LG detected by us in the cytoplasm of the

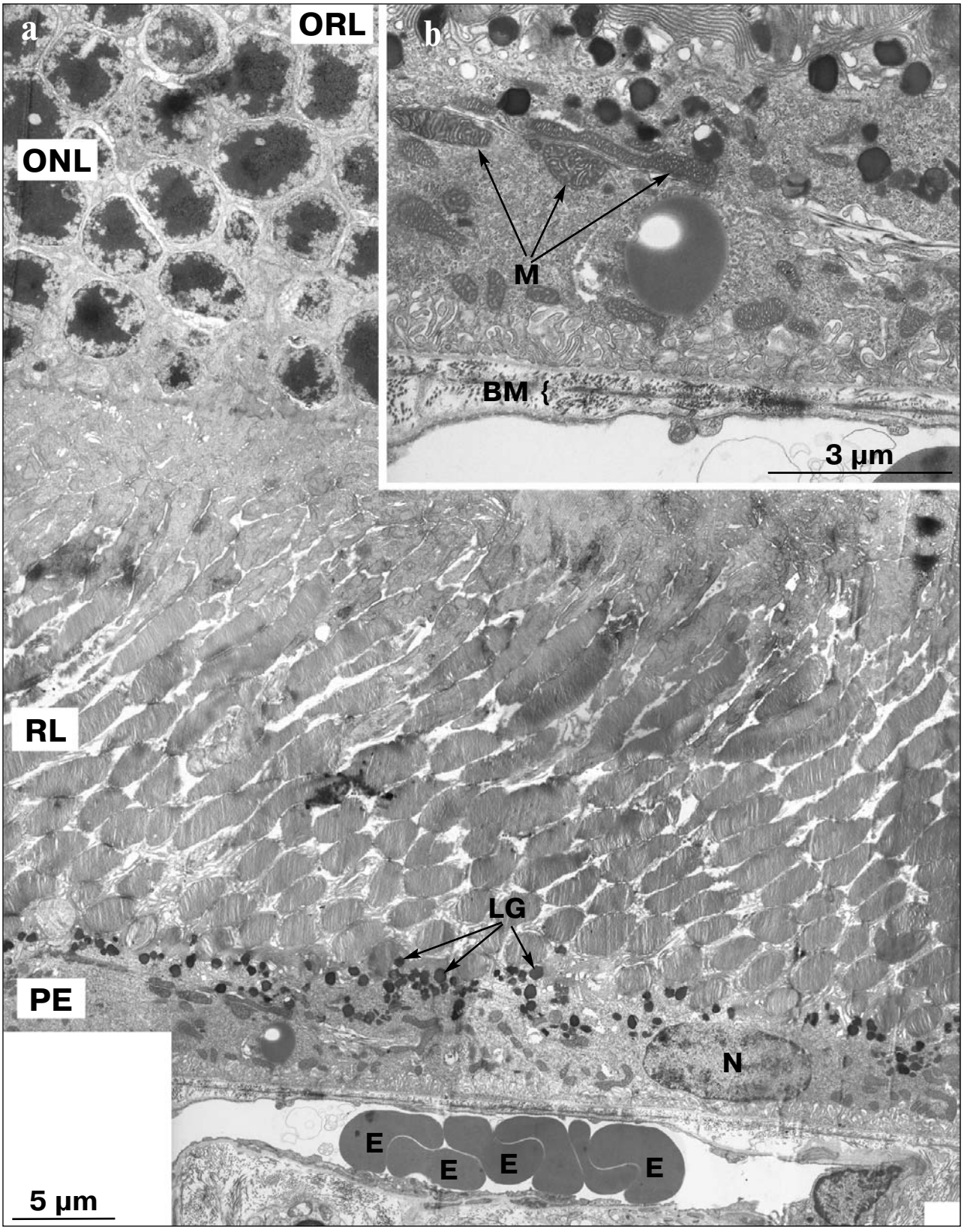

Fig. 8. Electron micrographs of a segment of the retina of a 24-month-old OXYS rat that received SkQ1 (250 nmol/kg) daily with food during five months. a) Summary photography. ORL, outer reticular layer; ONL, outer nuclear layer; RL, rod layer; PE, pigmented epithelium; N, nucleus of PE cell; E, erythrocytes; LG, lipofuscin granules. b) Specific features of ultrastructure of PE cell and of BM. M, mitochondria; BM, Bruch's membrane.

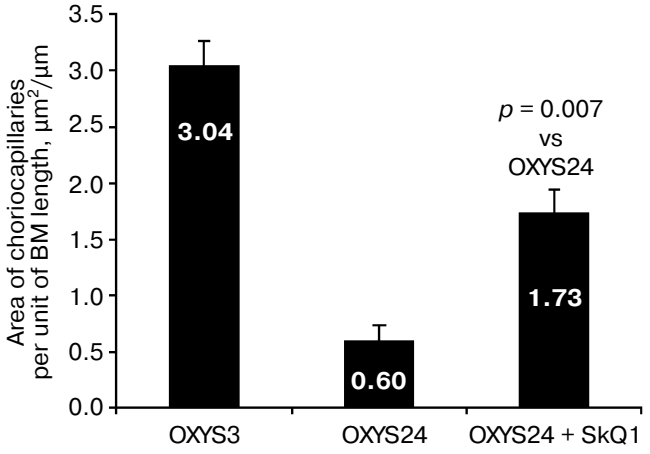

Fig. 9. Area of choriocapillaries per unit of BM length (μm²/μm) in 3-month-old OXYS rats (OXYS 3), 24-month-old OXYS rats (OXYS 24), and 24-month-old OXYS rats treated with SkQ1 (OXYS 24 + SkQ1) ($p = 0.007$, STATISTICA 6).

pigmented epithelium cells represents this process and promotes the development of further disorders in visual cycle functioning because LG are known to be very phototoxic [15]. The virtually full absence of phagosomes in the pigmented epithelium also speaks in favor of this hypothesis.

Changes in the CCL are typical for both Wistar and OXYS rats. However, the ultrastructural state of the CCL of 24-month-old Wistar rats indicates that it is a functioning structure and its disorders are not as significant as in 24-month-old OXYS rats. We have not found a complete obliteration of vessels in Wistar rats, and the mathematical processing confirmed these observations. In fact, in 24-month-old Wistar rats the specific area of choriocapillaries per BM length unit is 1.08 ± 0.22 μm²/μm, whereas in OXYS rats this parameter is only 0.6 ± 0.13 μm²/μm. Our findings correlate with data of Kolosova et al. [31] that related dystrophic changes in the retina macular region were observed in 92% of OXYS rats already in the age of 11 months, whereas in Wistar rats similar changes were recorded only in some animals (7%) and at 12 months.

Our study by electron microscopy has shown that treatment with SkQ1 restores the PE ultrastructure to the state characteristic for this tissue in rats without vision disorders. Moreover, SkQ1 not only arrests the development of degenerative changes in BM ultrastructure specific for affected animals but restores the ultrastructure of this complex.

The treatment with SkQ1 significantly increased the specific area of functioning choriocapillaries in the rats of both strains. In the antioxidant-treated Wistar rats this area was twofold (2.22 ± 0.35 and 1.08 ± 0.22 μm²/μm, respectively) and in OXYS rats 2.8-fold higher (1.73 ± 0.21 and 0.6 ± 0.13 μm²/μm, respectively) than in the control animals. This finding is rather impressive because a virtually complete degradation of the CCL in the untreated animals seemed to exclude the possibility of any recovery of the completely lost system of small vessels.

Thus, our study by electron microscopy has shown on the ultrastructural level the powerful therapeutic effect of the mitochondria-targeted antioxidant SkQ1. The treatment of Wistar and OXYS rats from the age of 19 months prevented disorders and/or recovered structural and functional parameters of choriocapillaries, PE, and BM. It is principally important that the therapeutic effect of SkQ1 was observed on Wistar and OXYS rats with pronounced age-related changes in the retina. The mathematical processing and statistical analysis fully confirmed the visually recorded age-related changes in the ultrastructure of choriocapillaries of the retina of Wistar and OXYS rats.

REFERENCES

1. Hayashi, A., Majji, A. B., Fujioka, S., Kim, H. C., Fukushima, I., and de Juan, E., Jr. (1999) *Graefes Arch. Clin. Exp. Ophthalmol.*, **237**, 668-677.
2. Henkind, P., and Gartner, S. (1983) *Trans. Ophthalmol. Soc. UK*, **103**, 444-447.
3. Heriot, W. J., and Machemer, R. (1992) *Graefes Arch. Clin. Exp. Ophthalmol.*, **230**, 91-100.
4. Leonard, D. S., Sugino, I. K., Zhang, X. G., Ninomiya, Y., Yagi, F., Tsukahara, I., Castellarin, A., and Zarbin, M. A. (2003) *Exp. Eye Res.*, **76**, 473-491.
5. McLeod, D. S., Grebe, R., Bhutto, I., Merges, C., Baba, T., and Lutty, G. A. (2009) *Invest. Ophthalmol. Vis. Sci.*, **50**, 4982-4991.
6. Feigl, B. (2009) *Prog. Retin. Eye Res.*, **28**, 63-86.
7. Feigl, B. (2007) *Clin. Exp. Optom.*, **90**, 263-271.
8. Beatty, S., Koh, H., Phil, M., Henson, D., and Boulton, M. (2000) *Surv. Ophthalmol.*, **45**, 115-134.
9. Suzuki, M., Kamei, M., Itabe, H., Yoneda, K., Bando, H., Kme, N., and Tano, Y. (2007) *Mol. Vis.*, **23**, 772-778.
10. Ames, B. N., Shigenaga, M. K., and Hagen, T. M. (1993) *Proc. Natl. Acad. Sci. USA*, **90**, 7915-7922.
11. Cai, J., Nelson, K. C., Wu, M., Sternberg, P., Jr., and Jones, D. P. (2000) *Prog. Retin. Eye Res.*, **19**, 205-221.
12. Liang, F., and Godley, B. F. (2003) *Exp. Eye Res.*, **76**, 397-403.
13. Binder, S., Stanzel, V., Krebs, I., and Glittenberg, C. (2007) *Prog. Retin. Eye Res.*, **5**, 516-554.
14. Saprunova, V. B., Pilipenko, D. I., Alekseevsky, A. V., Fursova, A. Zh., Kolosova, N. G., and Bakeeva, L. E. (2010) *Biochemistry (Moscow)*, **75**, 130-138.
15. Ostrovsky, M. A. (2005) *Usp. Biol. Khim.*, **45**, 173-204.
16. Neroev, V. V., Arkhipova, M. M., Bakeeva, L. E., Fursova, A. Zh., Grigoryan, E. N., Grishanova, A. Y., Iomdina, E. N., Ivashchenko, Zh. N., Katargina, L. A., Kilina, O. V., Kolosova, N. G., Pilipenko, D. I., Kopenkin, E. P., Kovaleva, N. A., Novikova, Y. P., Filippov, P. P., Robustova, O. V., Saprunova, V. B., Senin, I. I., Skulachev, M. V., Sotnikova, L. F., Tikhomirova, N. K., Stefanova, N. A.,

Khoroshilova-Maslova, I. P., Tsapenko, I. V., Shchipanova, A. I., and Skulachev, V. P. (2008) *Biochemistry (Moscow)*, **73**, 1317-1328.
17. Zhdankina, A. A., Fursova, A. Zh., Logvinov, S. V., and Kolosova, N. G. (2008) *Byul. Eksp. Biol.*, **145**, 435-438.
18. Skulachev, V. P., Anisimov, V. N., Antonenko, Y. N., Bakeeva, L. E., Chernyak, B. V., Erichev, V. P., Filenko, O. F., Kalinina, N. I., Kapelko, V. I., Kolosova, N. G., Kopnin, B. P., Korshunova, G. A., Lichinitser, M. R., Obukhova, L. A., Pasyukova, E. G., Pisarenko, O. I., Roginsky, V. A., Ruuge, E. K., Senin, I. I., Severina, I. I., Skulachev, M. V., Spivak, I. M., Tashlitsky, V. N., Tkachuk, V. A., Vyssokikh, M. Y., Yaguzhinsky, L. S., and Zorov, D. B. (2009) *Biochim. Biophys. Acta*, **1787**, 437-461.
19. Markovets, A. M., Fursova, A. Z., and Kolosova, N. G. (2011) *PLoS One*, **6**, e21682.
20. Markovets, A. M., Saprunova, V. B., Zhdankina, A. A., Fursova, A. Zh., Bakeeva, L. E., and Kolosova, N. G. (2011) *Aging Albany N.Y.*, **3**, 44-54.
21. Menshikova, E. B., Shabalina, I. G., Zenkov, N. K., and Kolosova, N. G. (2002) *Byul. Eksp. Biol. Med.*, **133**, 207-210.
23. Rumyantseva, Y. V., Fursova, A. Zh., Fedoseeva, L. A., and Kolosova, N. G. (2008) *Biochemistry (Moscow)*, **73**, 1176-1182.
24. Solov'eva, N. A., Morozkova, T. S., and Salganik, R. I. (1975) *Genetika*, **11**, 63-71.
25. Young, R. W. (1988) *Surv. Ophthalmol.*, **32**, 252-269.
26. Winkler, B. S., Boulton, M. E., Gottsch, J. D., and Sternberg, P. (1999) *Mol. Vis.*, **5**, 32.
27. Imamura, Y., Noda, S., Hashizume, K., Shinoda, K., Yamaguchi, M., Uchiyama, S., Shimizu, T., Mizushima, Y., Shirasawa, T., and Tsubota, K. (2006) *Proc. Natl. Acad. Sci. USA*, **103**, 11282-11287.
28. Sun, H., Molday, R. S., and Nathans, J. (1999) *J. Biol. Chem.*, **274**, 8269-8281.
29. Kennedy, M. J., Lee, K. A., Niemi, G. A., Craven, K. B., Garwin, G. G., Saari, J. C., and Hurley, J. B. (2001) *Neuron*, **31**, 3187-101.
30. Sun, H., and Nathans, J. J. (2001) *Bioenerg. Biomembr.*, **33**, 523-530.
31. Kolosova, N. G., Lebedev, P. A., Fursova, A. Zh., Morozkova, T. S., and Gusarevich, O. G. (2003) *Usp. Gerontol.*, **12**, 143-148.